Particle Accelerators, 1996, Vol. 52, pp. 95–113
Reprints available directly from the publisher
Photocopying permitted by license only

A WAVEGUIDE OVERLOADED CAVITY AS LONGITUDINAL KICKER FOR THE DAΦNE BUNCH-BY-BUNCH FEEDBACK SYSTEM

R. BONI, A. GALLO, A. GHIGO, F. MARCELLINI,
M. SERIO and M. ZOBOV

INFN – Laboratori Nazionali di Frascati
P.O. Box 13, I-00044 Frascati (Roma), Italy

(Received 3 October 1995; in final form 20 December 1995)

The Φ-Factory DAΦNE is a 1020 MeV high luminosity e^+e^- circular collider under construction at the Frascati Laboratories of INFN. Multibunch operation (up to 120 bunches) is required to increase the collision rate and achieve the luminosity goal ($\approx 5 \cdot 10^{32}$ $cm^{-2}s^{-1}$).

The development of very efficient longitudinal and transverse bunch-by-bunch feedback systems is one of the fundamental items in the design and operation of the high-current storage rings. These systems are based on fast digital processing of the bunch position error to compute the proper energy correction to be transferred to the bunch itself. The energy transfer is made by means of dedicated devices (kickers) whose efficiency impacts directly the feedback system operation.

The design and prototype measurements of a new kind of longitudinal kicker based on a waveguide overloaded cavity instead of a more conventional stripline structure is presented here. A higher shunt impedance (almost a factor 2), corresponding to a higher device efficiency, together with a lower content of parasitic High Order Modes, has been obtained. On the other hand, being a standing wave, non-directional device, the cavity kicker delivers beam coupled power to the input ports and broadband circulators have to be interposed to protect the kicker driving amplifiers.

Keywords: Kickers, feedback systems, impedances

1 INTRODUCTION

The multibunch operation of DAΦNE, and in general of any "factory" machine, calls for a very efficient feedback system to damp the coupled-bunch longitudinal instabilities. A collaboration program among SLAC, LBL and LNF laboratories on this subject[1] led to the development of a time domain, digital system based on digital signal processors (DSP) that has been already successfully tested at ALS.

The feedback chain ends with the longitudinal kicker, an electromagnetic structure capable of transferring the proper energy correction to each bunch.

The kicker design has to be optimised mainly with respect to the following parameters: the shunt impedance (i.e. the ratio between the square of the kick voltage and the peak forward power at input), the bandwidth ($f_{RF}/2$ required at least to damp any coupled-bunch mode) and the content of High Order Modes that can further excite coupled-bunch instabilities.

A stripline based design has been already proposed and adopted for ALS;[2] it consists of a pair of coaxial (with respect to the vacuum vessel) quarter-wavelength electrodes series connected through a half-wavelength delay line. Even though this solution can meet our impedance and bandwidth specifications, we have learned from experience on a prototype that proper tuning and matching is not simple and requires several iterations; moreover such kind of structures shows a worrisome content of undamped HOMs.

Therefore, we have explored the possibility of using an "overdamped" RF cavity as longitudinal kicker, in the same fashion as the DAΦNE main ring cavity[3] except that in this case the waveguide coupling has been enhanced and extended to the fundamental mode to enlarge its bandwidth. The strong waveguide coupling leads also to a remarkable damping of all the cavity HOMs.

Since the modelling of this structure is simpler than that of a stripline based kicker, the field solutions are easier to calculate, so that in this case we can rely on a design based on 3D simulations performed with the Hewlett-Packard code HFSS.[4]

The result of the design simulation together with some encouraging preliminary measurement performed on a prototype built at LNF are presented and discussed in this paper.

2 DESIGN OF THE OVERDAMPED CAVITY

A cut-view of the final geometry of the overdamped cavity proposed as longitudinal kicker is shown in Figures 1a and 1b. The very large bandwidth required has been obtained by strongly loading a pill-box cavity with special ridged waveguides followed by broadband transitions to 7/8" standard coaxial. Ceramic feedthroughs allow in-air connections to the driving amplifiers (input ports) and dummy loads (output ports).

An exploded 180° cut-view is shown in Figure 1a, where the basic pill-box cavity and the waveguides together with the transitions to coaxial line are clearly recognizable, while a cut-view of the whole kicker assembly is shown in Figure 1b. The waveguides are placed on both cavity sides symmetrically with respect to the field distribution of the operating mode. Due to this symmetry it turns out that, if the ports on one side are driven in phase with balanced levels and the ports on the opposite side are connected to dummy loads, the system in principle is perfectly

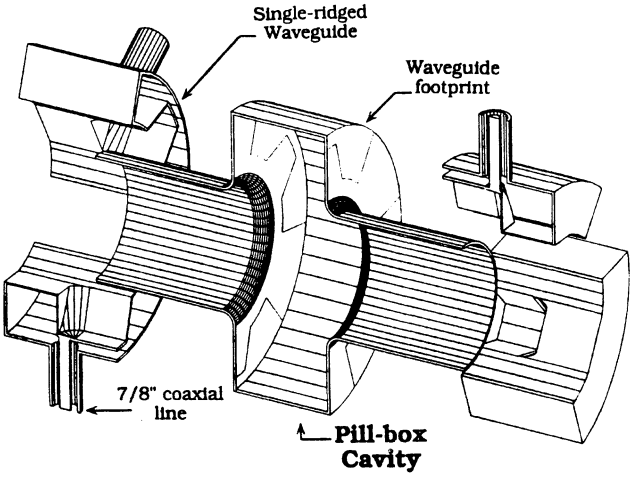

FIGURE 1a: Longitudinal kicker exploded cut-view.

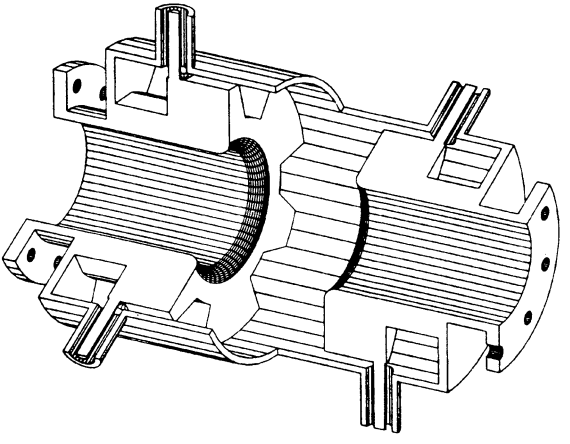

FIGURE 1b: Longitudinal kicker assembly cut-view.

matched at its central frequency, i.e. no power is reflected at that frequency by the input ports.

Moreover the cavity, being broadband, does not need to be tuned nor cooled, since almost all the power is dissipated in the external loads.

The idea of using an RF cavity as longitudinal kicker is based on some simple considerations. When all the RF buckets are filled, all possible coupled bunch

modes are present in a frequency span between nf_{RF} and $(n + 1/2)f_{RF}$, with n any integer. Therefore, without an *a priori* knowledge of the position of the most dangerous HOMs, the minimum bandwidth requirement for the longitudinal kicker is $f_{BW} = f_{RF}/2$, as long as the response is centered onto $f_c = (n + 1/4)f_{RF}$. A center frequency $f_c = 3.25\ f_{RF} \approx 1197$ MHz has been chosen so that the resulting loaded quality factor of the cavity has to be set to about $Q_L = fc/f_{BW} \approx 6.5$. Therefore, if the damping waveguides are symmetrically placed with respect to the fundamental mode field distribution and half of them are used as input ports while the remaining as matched terminations, the external Q values are given by:

$$Q_{\text{ext}_{\text{inp}}} \approx Q_{\text{ext}_{\text{out}}} \approx 2Q_L \approx 13 \tag{1}$$

The R/Q factor of a pill-box cavity resonating at around 1.2 GHz with stay-clear apertures of 88 mm is limited to about 60 Ω. The kicker shunt impedance R_s has a peak value given by:

$$R_s = V_k^2/2P_{\text{in}} \approx (R/Q)Q_{\text{ext}_{\text{out}}} \approx 780\ \Omega \tag{2}$$

This means that the attainable shunt impedance is about twice the value of a two-electrodes stripline module,[2] while no HOMs are likely to remain undamped in this structure.

The cavity design has been based on the pill-box cavity profile sketched in Figure 2. The pill-box modes up to the beam pipe cutoff computed by the 2D code URMEL[5] are shown in Table 1. The Q values reported refer to Copper cavity walls. Due to the large size of the stay-clear apertures, there was very little margin for the optimisation of the R/Q factor, so that we accepted to base the design on a simple pill-box shape instead of a more complex nosecone geometry.

As a second step, the shape of the loading waveguides has been defined. The waveguide cross-section and the pill-box side view are shown in Figure 3. It is a single ridged like waveguide with 6 mm gap to lower the TE10 cutoff frequency down to 690 MHz. As described in the following, a low cutoff frequency makes

TABLE 1: Summary of the pill-box modes as given by the code URMEL.

Mode	0-EM-1	0-MM-1	0-EM-2	1-EM-1	1-MM-1
f [MHz]	1227.06	2421.81	2663.60	1729.00	1750.29
Q	22318	20533	41260	23645	25101
R/Q [Ω]	54.696	5.129	0.132	17.979	2.888

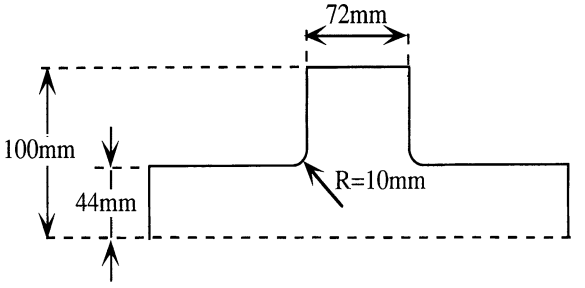

FIGURE 2: Pill-box profile.

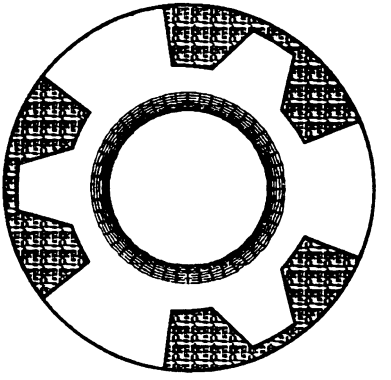

FIGURE 3: Waveguide cross-section on cavity wall.

the conversion of the TE10 waveguide mode to the coaxial TEM mode in a wide frequency range easier.

The coaxial size is the standard 50 Ω, 7/8" which can withstand more than 1 KW power flow. Moreover, we can use for this coaxial standard the broadband ceramic feedthrough already developed for the transitions of the main ring cavity.[7]

The reflection frequency response of the transition computed with HFSS is shown in Figure 5. The S_{11} value is lower than 0.25 along the entire frequency band up to the beam pipe cut-off; the low cut-off frequency of the TE10 mode of the waveguide ($\approx$ 690 MHz) is crucial to get a good wave transmission in the low frequency band.

The cross-section area of each waveguide covers about 11% of the available surface of the pill-box side and up to 4 waveguides can be applied on each cavity side. Actually, only 3 waveguides per side are enough to get a Q_L value lower than 6.5 and a bandwidth larger than $f_{RF}/2$, as shown in the following.

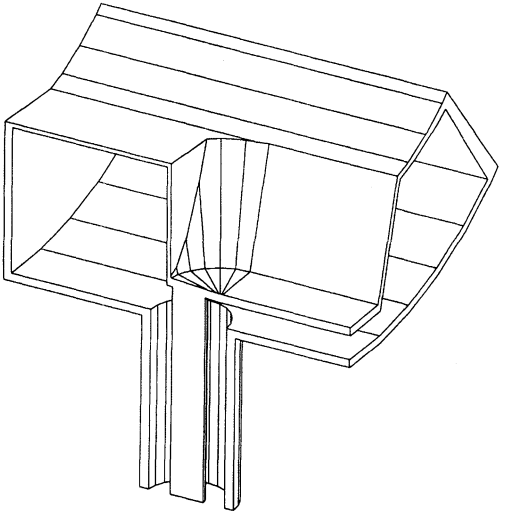

FIGURE 4: Broadband transition sketch (section view).

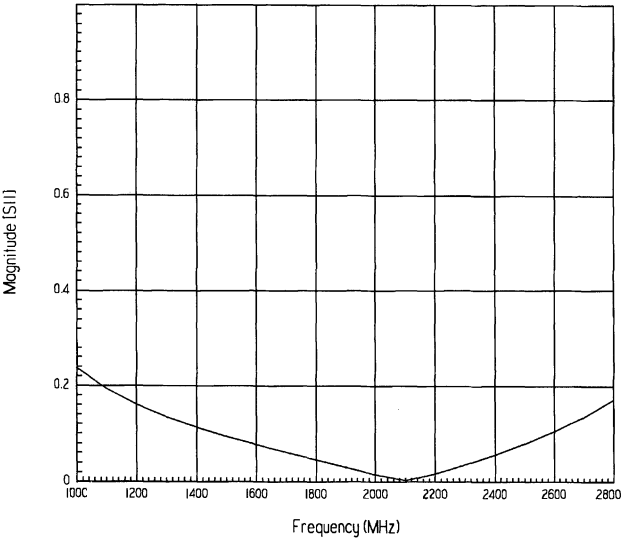

FIGURE 5: Transition frequency response (HFSS simulation).

Once the shape of the damping waveguides had been defined, we designed the waveguide-to-coaxial transition with the same criteria adopted for the main ring cavity.[6]

A cut-view sketch of the loading waveguide together with the transition to coaxial line is shown in Figure 4. The waveguide ridge is truncated with a round section where the coaxial inner conductor is connected; a short-circuited waveguide section behind the coaxial insertion (the so called "back cavity") helps in centering the transition frequency response.

The kicker geometry shown in Figure 1 is the assembly of the pill-box cavity with three equally spaced broadband transitions of the kind sketched in Figure 4 per side.

A full scale Aluminium prototype of the kicker cavity has been manufactured at LNF in order to get an experimental proof of the computer simulation results. A picture of the inside view half of the prototype structure is shown in Figure 6. The prototype is only suitable for low-power, in-air measurements.

3 COMPUTER SIMULATIONS AND EXPERIMENTAL RESULTS

3.1 Frequency Response

The transmission coefficient S_{21} from the three input ports to the three output ports for the cavity fundamental mode is shown in Figure 7. The solid line represents the computed response and has a peak at about 1215 MHz and a bandwidth as large as 220 MHz.

The measured transmission coefficient is represented by the dashed line showing approximately the same bandwidth around a center frequency of about 1209 MHz. The shape of the measured frequency response appears to be a little distorted. This is probably due to the mechanical imperfections of the prototype since the response has been found to be very sensitive to any mechanical or electrical difference among the six input/output channels.

The computed and measured frequency response of the two dipole modes 1EM1 and 1MM1 is shown in Figure 8. The 1EM1 mode is strongly damped ($Q_L \approx 16$ in both simulations and measurements). The resulting peak transverse impedance $R_\perp$(1EM1) is about 300 Ω while the "actual" transverse impedance, that takes into account the beam spectrum roll-off and the form factor corresponding to a 3 cm bunch length, is reduced to about 125 Ω.

The 1MM1 dipole is less damped than the 1EM1. The simulations give a Q_L value of about 500 corresponding to 1400 Ω and 550 Ω of peak and "actual" impedances respectively. In this case the measured Q_L seems to be a factor 3 lower than the computed value and the impedance values should scale accordingly by the

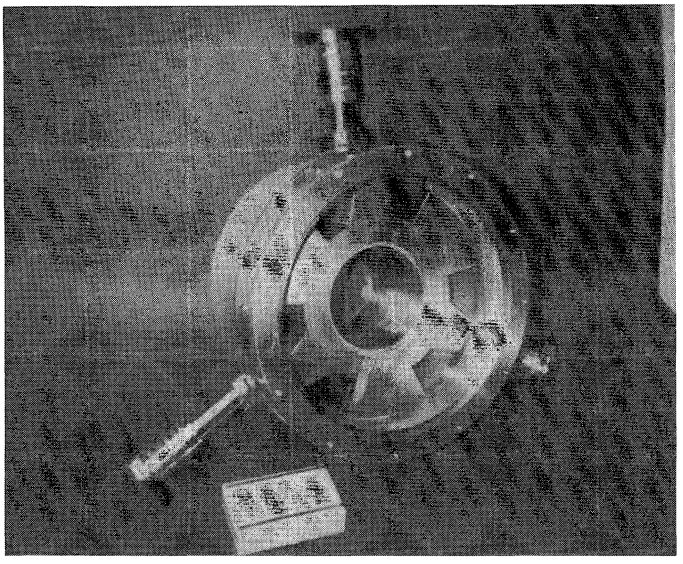

FIGURE 6: Kicker cavity prototype.

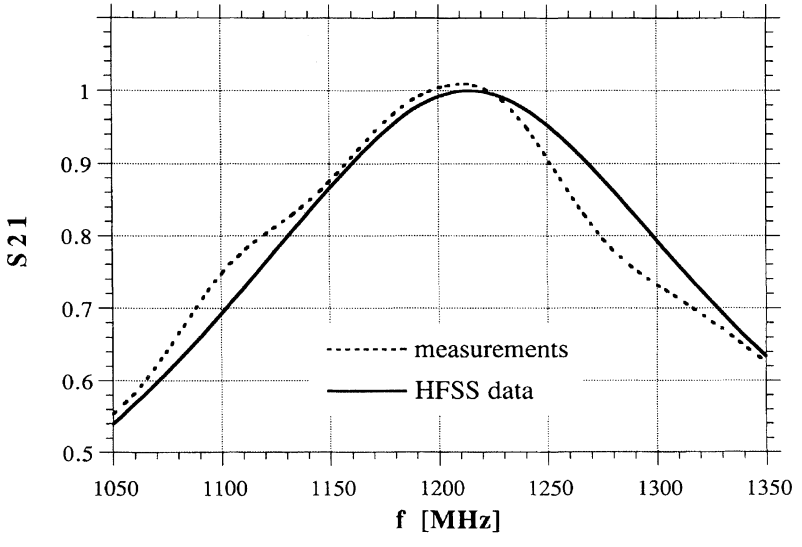

FIGURE 7: Kicker frequency response.

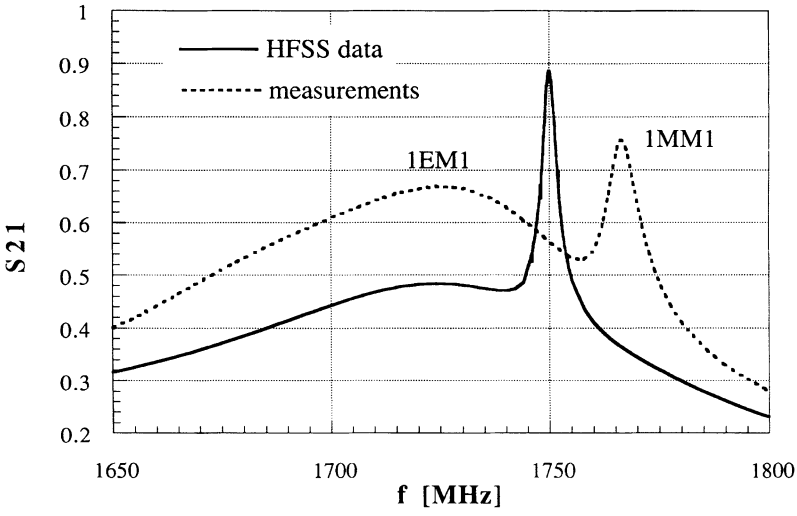

FIGURE 8: Dipolar mode frequency response.

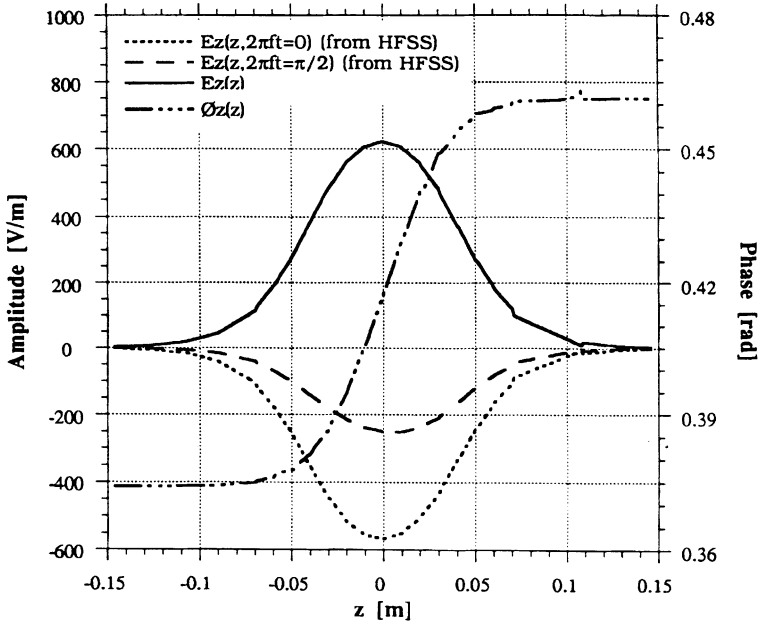

FIGURE 9: Longitudinal E-field on beam axis.

same factor. However, the contribution of this mode to the machine transverse instability (rise time $\tau_T \geq 4.5$ msec in full coupling and 30 bunches) is at most comparable to the contribution of the first dipole modes of the DAΦNE main ring cavity, that are considered not dangerous for the transverse dynamics.[8]

The 0MM1 monopole mode, mentioned in Table 1, looks extremely damped in the HFSS simulations ($Q_L \approx 10$) while it is not clearly detectable and measurable from prototype port-to-port transmission measurements.

The 0EM2 monopole mode reported in Table 2 has not been found both in the 3D simulations and measurements probably because it penetrates deeply in the drift tubes since its resonant frequency is very close to the beam pipe cut-off.

3.2 Shunt Impedance Calculation and Measurements

The most important figure of merit of the kicker is the shunt impedance R_s defined as:

$$R_s = \frac{|V_g|^2}{2P_{fw}} \tag{3}$$

where V_g is the kicker gap voltage as seen by a relativistic particle, and P_{fw} is the forward power at kicker input. The only straightforward way to compute the shunt impedance is to post-process the field solution given by the 3D simulator. In fact, the gap voltage V_g may be obtained by integrating the longitudinal E-field on the beam axis including in the integration of the transit time factor.

What one can get from the HFSS field solution is the value of the fields at the solution frequency and at the desired phase. The longitudinal E-field on the beam axis computed by HFSS at 1.2 GHz and 1 W forward input power is shown in Figure 9 at 0 and $\pi/2$ phases, taking the forward wave at the input ports as the phase reference.

In order to compute the shunt impedance R_s it is convenient to represent the longitudinal E-field as a phasor, namely:

$$E_z(z,t) = \mathrm{Re}\left\{E_z(z)\, e^{j[\omega t - \phi_z(z)]}\right\} \tag{4}$$

where the two functions $E_z(z)$ and $\phi_z(z)$ can be obtained from the field solutions according to:

$$\begin{aligned} E_z(z) &= \sqrt{E_z^2(z, \omega t = 0) + E_z^2(z, \omega t = \pi/2)} \\ \phi_z(z) &= \mathrm{Atan}\left[\frac{E_z(z, \omega t = \pi/2)}{E_z(z, \omega t = 0)}\right] \end{aligned} \tag{5}$$

Accordingly to (4) and (5), the function $\phi_z(z)$ depends on the choice of the phase reference only for a constant offset, while the function $E_z(z)$ is totally independent from that choice.

Once the functions $E_z(z)$ and $\phi_z(z)$ have been computed at a certain frequency, the gap voltage as a complex phasor is given by:

$$V_g(\omega) = \int_{-L/2}^{L/2} E_z(z)\, e^{j[\omega z/c - \phi_z(z)]} dz \tag{6}$$

where L is the cavity length and the term $\omega z/c$ in the exponential accounts for the transit time effect.

The amplitude and phase of the phasor $V_g(\omega)$ is plotted in Figure 10 for 7 different frequencies, while the shunt impedance $R_s(\omega)$, given by Equation (3), is shown in Figure 11. The impedance peak value is about 750 Ω, in good agreement with the rough estimate (2).

It is interesting to remark that the impedance peak value occurs at about 1.2 GHz, i.e. 15 MHz below the transmission peak response, and that the high frequency portion of the plot decreases more rapidly than the low frequency one. Both effects are due to the fact that, since we are considering a wide frequency band, the transit time factor is no longer a constant but decreases linearly with frequency.

The shunt impedance of the cavity prototype has been measured with the wire method. A 3 mm diameter Copper rod, mechanically supported by special, non-reflective stand-offs, has been inserted in the cavity along the beam axis and connected to a 50 Ω line through a resistive matching network. The coaxial rod-beam tube system is a $Z_0' = 203$ Ω transmission line and the matching network task is to adapt it to the 50 Ω input/output ports. The longitudinal beam impedance $Z(\omega)$, defined as the complex ratio between the cavity gap voltage and the beam current, can be calculated[9] with some approximation, according to:

$$Z(\omega) \approx 2Z_0' \left(\frac{1}{S_{21}} - 1 \right) \tag{7}$$

where S_{21} is the complex transmission coefficient between the 2 beam tube ports measured by a Network Analyzer accurately calibrated to take into account the cable and matching network attenuations, as well as the linear phase advance due to the electrical length of the device.

The quality of the matching is crucial to eliminate or reduce spurious resonances in the frequency response arising from the TEM wave reflections at the step transition between the 50 Ω and 203 Ω coaxial lines.

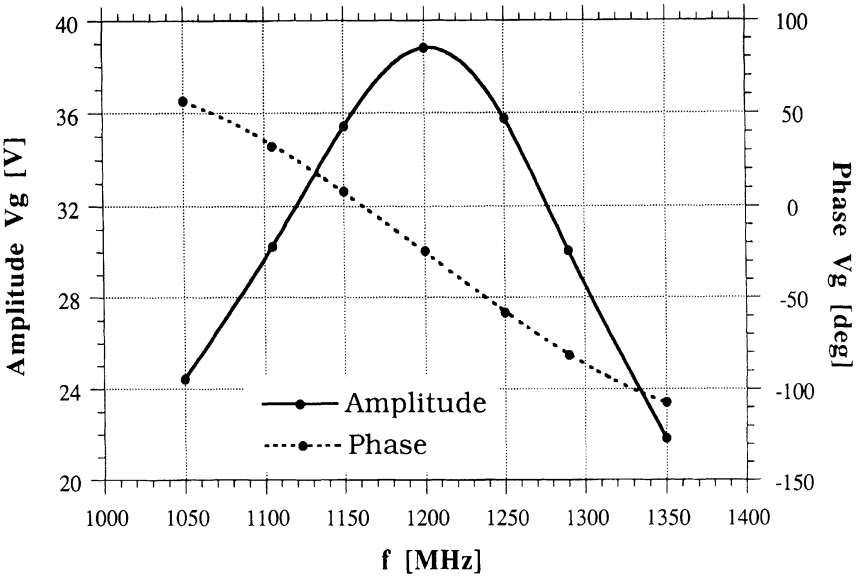

FIGURE 10: Gap voltage (P_{in}=1 W).

The reflection coefficient measured at the step transition with and without the resistive matching network is shown in Figure 12 (solid and dashed line respectively). The dashed line shows a return loss value of about −4 dB all over the measurement bandwidth, corresponding to a 50 Ω line terminated with a 200 Ω resistor. The solid line, i.e. the matched case, shows a substantially lower return loss value increasing with frequency and limited to about −17 dB in the measurement bandwidth (1 ÷ 1.5 GHz).

The amplitude and phase of the transmission coefficient S_{21} measured with the already mentioned calibration factors is shown in Figure 13. The amplitude minimum, corresponding to the peak power absorption of the device and therefore to the impedance peak value, is located at about 1325 MHz. This means that the rod perturbs the field distribution and shifts the resonant frequency by about +125 MHz.

By applying the simple formula (7) on the data taken with the measurement of Figure 13 the longitudinal beam impedance shown in Figure 14 has been obtained. Both real and imaginary parts of the impedance can be very well fitted by an R-L-C lumped resonator.

The shunt impedance, as defined in (3), turns out to be twice the value of the real part of the beam impedance. In Figure 15 the dashed line represents the shunt impedance obtained from the wire measurements, while the solid line is a HFSS

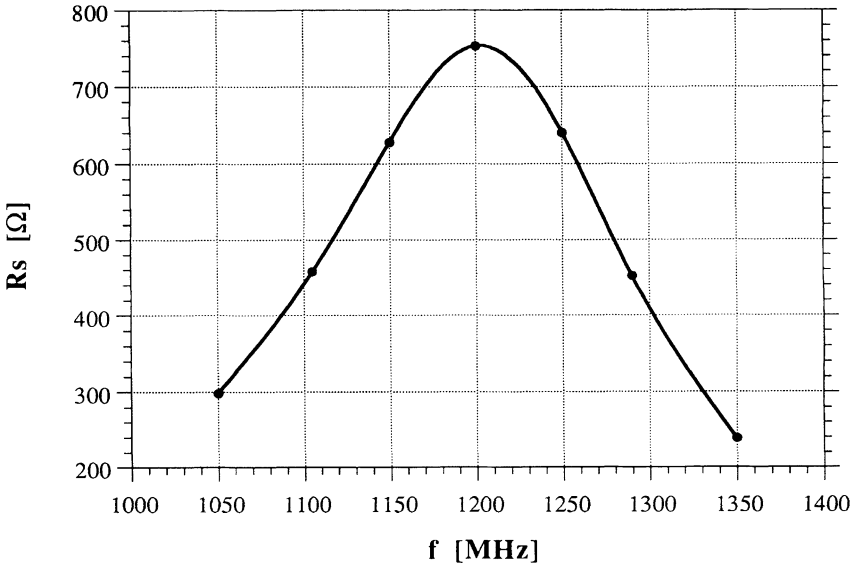

FIGURE 11: Kicker shunt impedance.

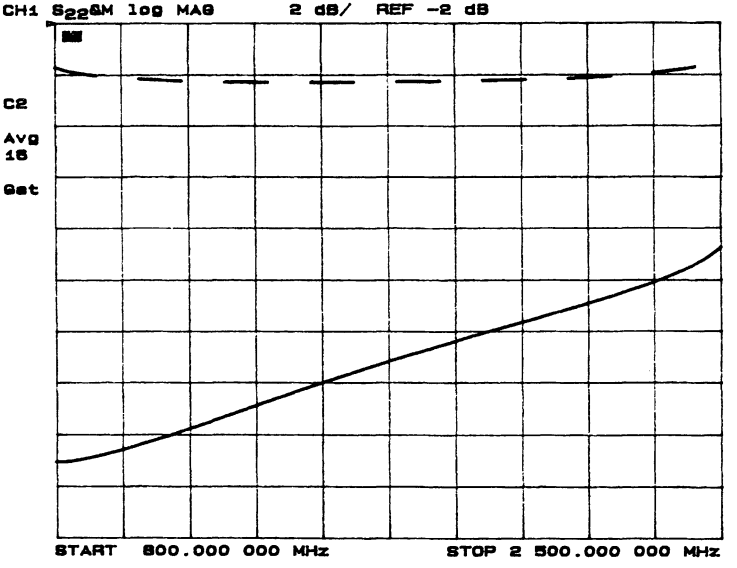

FIGURE 12: Matching network effect on step transition return loss.

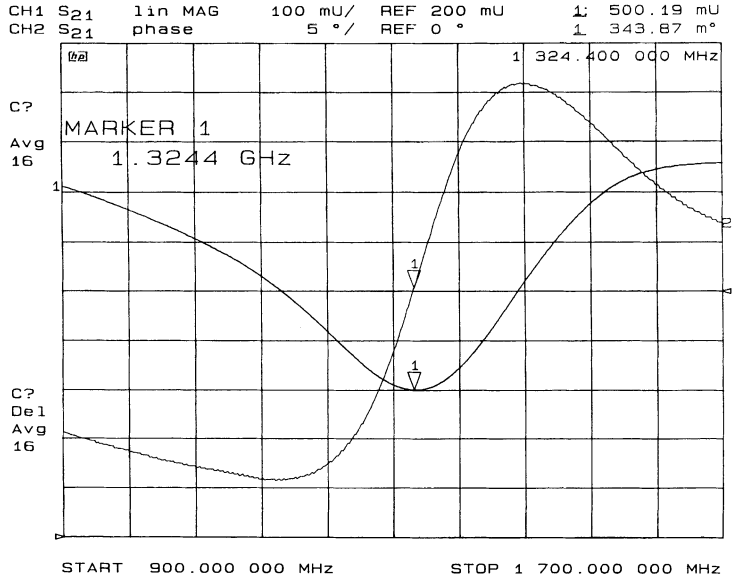

FIGURE 13: Wire measurement transmission response.

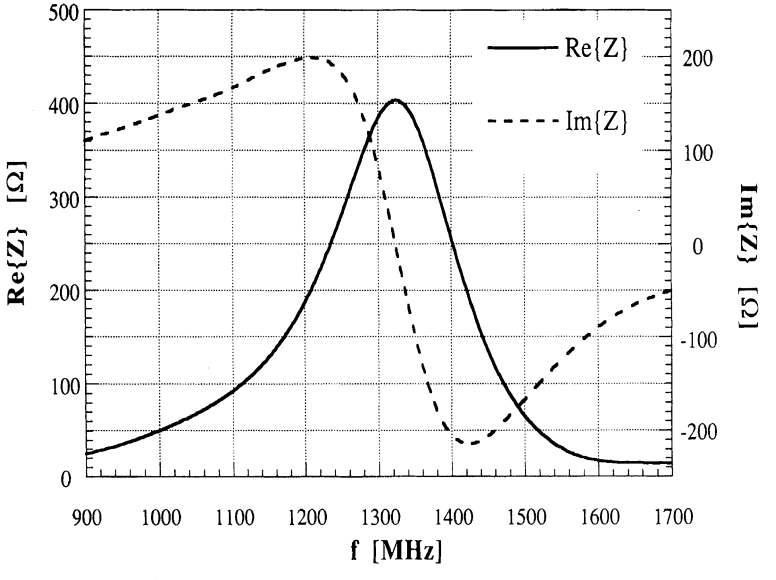

FIGURE 14: Beam coupling impedance measured on the kicker prototype.

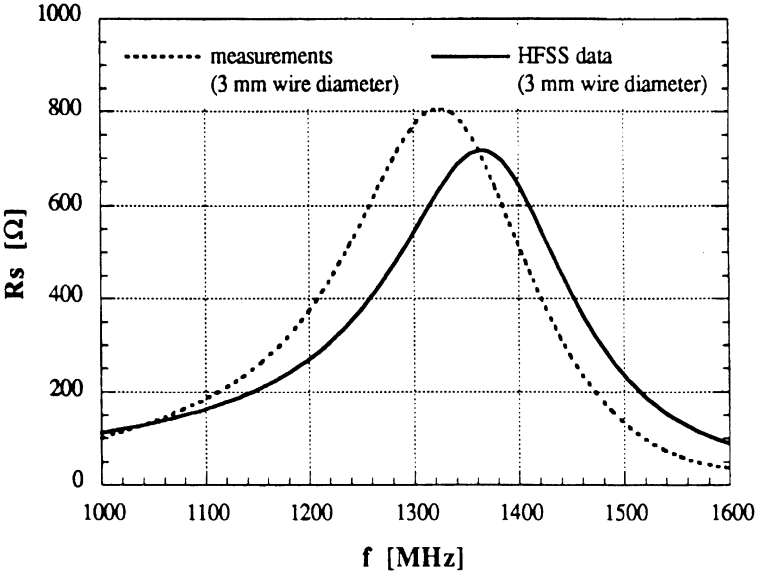

FIGURE 15: Kicker shunt impedance obtained with the wire method.

simulation of the wire measurement. The measurement and simulation curves are in rather good agreement and show a similar frequency shift value (+125 and +160 MHz respectively) and a peak value of 800 Ω and 720 Ω respectively that confirm the data of the Figure 11 plot. However, by reducing the wire diameter in the simulations, a lower shift value and a higher impedance have been obtained, in better agreement with the experimental results.

The contribution of the basic pill box of Figure 2 to the machine broadband impedance has been estimated by means of the ABCI code.[10] The longitudinal and transverse loss factors k_l and k_T of the device for a 3 cm bunch length are $\approx$ 0.12 V/pC and $\approx$ 3.5 V/pC m respectively. With respect to a two-electrode stripline module, the k_l value is comparable while the k_T value is about 50% lower. It must be pointed out, however, that such a module can only provide half of the kicker cavity shunt impedance.

4 POWER CONSIDERATIONS

According to simulations, DAΦNE operation will require a maximum longitudinal kick voltage of $\approx$ 400 V with 30 bunches and 1600 V with 120 bunches in order to

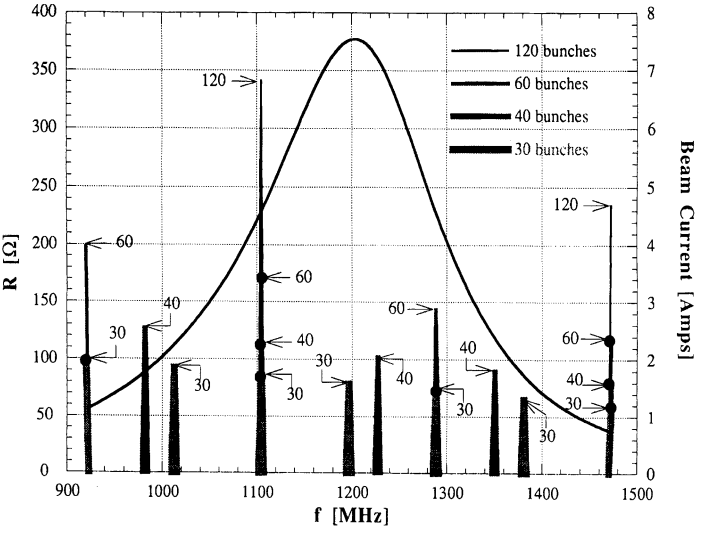

FIGURE 16: Beam spectrum and cavity coupling impedance.

damp an initial offset of 100 psec, a prudent estimate of the maximum injection error of the last bunch. A 200 W input power with a single kicker cavity per ring will be enough for the 30 bunch operation while 2 kickers per ring fed with 600 W each will be eventually required for the 120 bunch operation.[3]

On the other hand, the beam current interacts with the device beam impedance, and the power released by the beam can be much higher than the incoming power from the feedback system. The plot of the kicker beam impedance real part and various configurations of the beam current spectrum are shown in Figure 16. The total power P_b released by the beam for a certain current spectrum configuration is given by:

$$P_b = \sum_n \frac{1}{2} \mathrm{Re}[Z(\omega_n)] I_n^2 \tag{8}$$

so that the resulting power rates are reported in Table 2. The beam spectra shown in Figure 16 include the effect of the roll-off due to the 3 cm DAΦNE bunch length.

TABLE 2: Power released to the cavity by various DAΦNE beam configurations.

Number of regularly spaced bunches	30	40	60	120
Total Power [W]	2500	3200	4800	9600
Power per guide [W]	420	530	800	1600

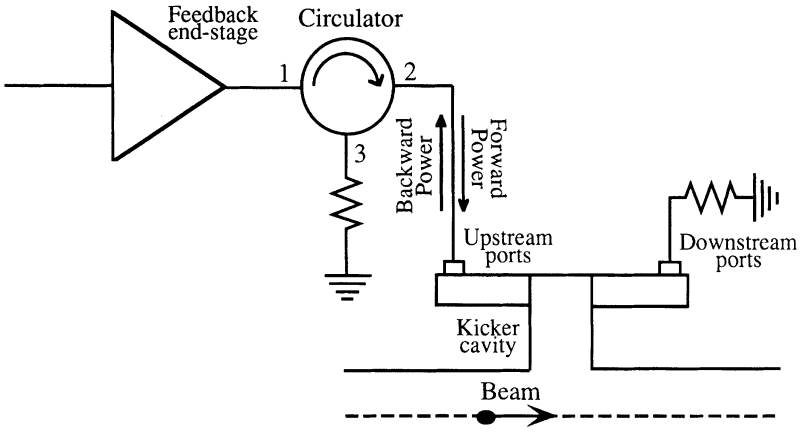

FIGURE 17: Sketch of the longitudinal feedback system back-end.

Being mainly a standing wave structure, the cavity kicker is not a directional device and upstream and downstream ports are almost equally coupled to the beam. Therefore, unlike the case of the stripline based kicker, in the cavity the beam power reaches indifferently the input and output ports. The longitudinal feedback power amplifiers must be protected with ferrite circulators against the backward power released by the beam that can be one order of magnitude higher than the forward level. A sketch of the longitudinal feedback system back-end is shown in Figure 17.

A preliminary market investigation has proven that a custom ferrite circulator covering a band wider than the $1 \div 1.4$ GHz range at a power rate of 1.5 kW with an isolation higher than 18 dB can be certainly developed.[11] The plot of the circulator scattering matrix elements as preliminary computed by a lossless simulation (courtesy of the AFT company) is shown in Figure 18. The port 1 is more than 20 dB isolated from port 2 in the operating bandwidth, so that less than 1% of the power released by the beam can actually reach the feedback end-stage amplifier. On the other hand the circulator response shows a resonance around 1550 MHz that should not affect the kicker behaviour since it does not overlap neither the fundamental nor the kicker HOMs.

5 CONCLUSIONS

A cavity kicker for the DAΦNE bunch-by-bunch longitudinal feedback system based on a pill-box loaded by six waveguides has been designed and a full-scale Aluminium prototype has been fabricated at LNF. Both simulations and

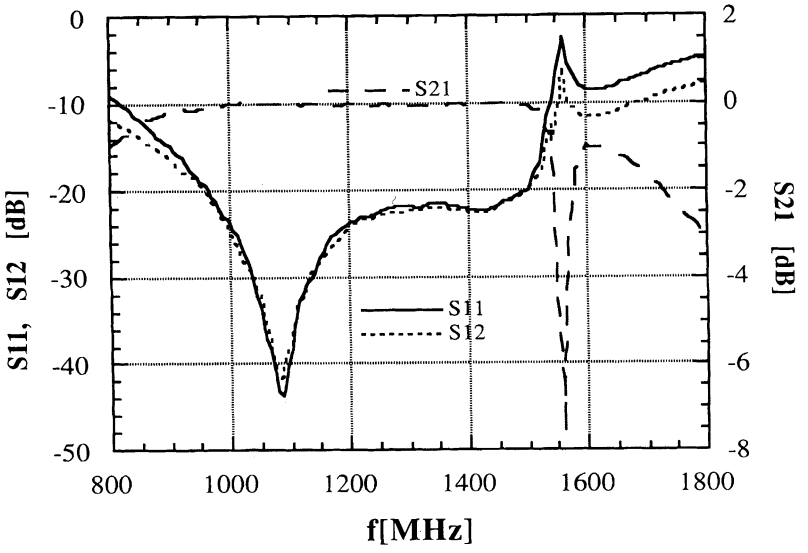

FIGURE 18: Circulator scattering matrix elements (courtesy of AFT Co).

measurements have shown a peak shunt impedance of about 750 Ω and a bandwidth of about 220 MHz. The large shunt impedance allows to economise on the costly feedback power. Moreover the damping waveguides drastically reduce the device HOM longitudinal and transverse impedances.

The feedback signal can enter the cavity from the coaxial ports attached to the waveguides so that no special input coupler is required. Due to the large bandwidth and low internal dissipation, neither tuning nor cooling is necessary.

The mechanical specifications and drawings of the vacuum compatible cavity have been finalised and an order for two pieces (one per ring) has been placed already. The fabrication of the two devices is well in progress.

One cavity per ring will be sufficient to operate the machine up to 30 bunches while a second device per ring together with a feedback power improvement will be necessary to reach the ultimate current.

Acknowledgements

The authors wish to thank M. Migliorati, L. Palumbo and B. Spataro for the continuous opinion exchange on the subject. Thanks also to D. Boussard and all the DAΦNE machine reviewers who have revised a preliminary version of this

work. Thanks to S. Quaglia for his help in the computer acquisition of the RF measurements. The authors are especially indebted with T. Tranquilli who worked hard to mechanically design and fabricate a very good kicker prototype in a very short time. Thanks also to P. Baldini and M. Scampati who helped him in many ways.

References

[1] J.D. Fox, *et al.*, "Operation and Performance of a Longitudinal Damping System Using Parallel Digital Signal Processing", in *Proceedings of the 4th EPAC*, London, 1994, p. 1619.
[2] J.N. Corlett, *et al.*, "Longitudinal and Transverse Feedback Kickers for the ALS", in *Proceedings of the 4th EPAC*, London, 1994, p. 1625.
[3] G. Vignola and the DAΦNE Project Team, "DAΦNE Status and Plans", in *Proceedings of Particle Accelerator Conference*, Dallas TX, May 1–5, 1995, in preparation.
[4] Hewlett-Packard Co, "HFSS, The High Frequency Structure Simulator HP85180A™".
[5] T. Weiland, Nucl. Instr. Methods, **216** (1983), pp. 329–348.
[6] R. Boni, *et al.*, "A Broadband Waveguide to Coaxial Transition for High Order Mode Damping in Particle Accelerator RF Cavities", *Particle Accelerator*, Vol. 45, 4 (1994), p. 195.
[7] R. Boni, *et al.*, "Update on the Broadband Waveguide to 50 Ω Coaxial Transition for Parasitic Mode Damping in the DAΦNE RF Cavities", in *Proceedings of the 4th EPAC*, London, 1994, p. 2004.
[8] M. Migliorati, private communication.
[9] H. Hahn and F. Pedersen, "On Coaxial Wire Measurements of the Longitudinal Coupling Impedance", BNL-50870, UC-28, April 1978.
[10] Y.H. Chin, "User's Guide for ABCI Version 8.8 (Azimuthal Beam Cavity Interaction)", LBL-35258, UC-414, February 1994.
[11] Advanced Ferrite Technology Co, Spinnerei 44, 71522 Backnang (FRG), private communication.